Are There Hydrogen Bonds in Supercritical Water?

Markus M. Hoffmann and Mark S. Conradi*

Contribution from the Departments of Physics and Chemistry—1105, Washington University, St. Louis, Missouri 63130-4899

Abstract: The proton NMR chemical shift has been measured for water from 25 to 600 °C and from 1 to 400 bar, conditions extending well beyond the critical point. Dilute solutes were employed as chemical shift references to avoid the effect of the varying magnetic susceptibility. The large changes in chemical shift (4.1 ppm) are interpreted as changes in the hydrogen bond network, because all other intermolecular interactions are known to result in much smaller effects. Using a linear relation between chemical shift and the mean number of hydrogen bonds, the NMR results show there are still 29% as many hydrogen bonds at 400 °C and 400 bar ($\rho = 0.52$ g/cm^3) as for room temperature water. The present results are compared to other measurements and calculations.

I. Introduction

Many of the unique properties of water are due, in large part, to its network of hydrogen bonds.[1−3] For example, H_2S and H_2Se have substantially lower boiling points than H_2O because H_2S and H_2Se form only weak H bonds, at best.[1,2] The tetrahedral arrangement of molecules in liquid water is similar to that in ordinary ice (-Ih) and serves to maximize the H bonding.[2,4] This unusually open structure leads to the well-known density maximum of water[5] at 4 °C. The high-pressure structures of solid H_2O, ices VII and VIII, have two interpenetrating, separate, ice-I-like sublattices;[4] this is striking evidence of the open structures of ice-I and, similarly, ordinary water. The large heat capacity of water and its substantial increase for $T < 0$ °C (supercooled) are also believed to be due to H bonds.[6−9]

Several recent developments have resulted in increased interest in supercritical water[10] (scw, generally taken as water above the temperature of the critical point; $T_c = 374$ °C, $P_c = 221$ bar, and $\rho_c = 0.32$ g/cm^3). Hazardous and toxic organics can be fully oxidized to innocuous end products[10−12] using scw as the reaction medium. Furthermore, organic waste can be partially transformed into light feedstocks[13] using scw. Super-

critical water is believed to be important in the geological formation of hydrocarbons, particularly methane.[14−17] New forms of life have been found at deep-sea hydrothermal vents;[18−20] the conditions at some of the vents are close to the critical point of water.[18] Massive deuteration of simple organics with very little auxiliary reaction has been found in near-critical and supercritical D_2O.[21] In addition, the study of supercritical water is relevant to the widespread use of supercritical (sc) solvents in reactions and separations.

It is crucial to an understanding of supercritical water to know to what extent H bonds persist in this fluid. This issue has been stimulated by a neutron diffraction study[22,23] using the isotopic substitution technique (NDIS).[24,25] These workers reported that H bonding was essentially absent at conditions (400 °C and 0.66 g/cm^3) just above the critical point. The interpretation of NDIS data is evidently nontrivial, since a reanalysis of the original data has been published.[26] Aside from the difficulty of extracting OO, HH, and OH pair distribution functions (e.g., $g_{OH}(r)$) from the raw data, it is unclear how to determine the extent of H bonds from the pair distribution functions. That is, it is not clear in the neutron data exactly

[⊗] Abstract published in *Advance ACS Abstracts,* April 1, 1997.

(1) Pimentel, G. C.; McClellan, A. L. *The Hydrogen Bond*; Freeman: San Francisco, CA, 1960.

(2) Eisenberg, D. S.; Kauzmann, W. *The Structure and Properties of Water*; Oxford: New York, 1969.

(3) Poole, P. H.; Sciortino, F.; Grande, T.; Stanley, H. E.; Angell, C. A. *Phys. Rev. Lett.* **1994**, *73*, 1632.

(4) Fletcher, N. H. *The Chemical Physics of Ice*; Cambridge: London, 1970; pp 70−85.

(5) Sato, H.; Uematsu, M.; Watanabe, K.; Saul, A.; Wagner, W. *J. Phys. Chem. Ref. Data* **1988**, *17*, 1439.

(6) Angell, C. A. In *Water: a Comprehensive Treatise*; Franks, F., Ed.; Plenum: New York, 1982; Vol. 7, Chapter 1.

(7) Rasmussen, D. H.; Mackenzie, A. P.; Angell, C. A.; Tucker, J. C. *Science* **1973**, *181*, 342.

(8) Angell, C. A.; Shuppert, J.; Tucker, J. C. *J. Phys. Chem.* **1973**, *77*, 3092.

(9) Sastry, S.; Debenedetti, P. G.; Sciortino, F.; Stanley, H. E. *Phys. Rev. E* **1996**, *53*, 6144.

(10) Shaw, R. W.; Brill, T. B.; Clifford, A. A.; Eckert, C. A.; Franck, E. U. *Chem. Eng. News* **1991**, *69* (51), 26.

(11) Harradine, D. M.; Buelow, S. J.; Dell'Orco, P. C.; Dyer, R. B.; Foy, B. R.; Robinson, J. M.; Sanchez, J. A.; Spontarelli, T.; Wander, J. D. *Haz. Waste Haz. Mater.* **1993**, *10*, 233.

(12) Killilea, W. R.; Swallow, K. C.; Hong, G. T. *J. Supercrit. Fluids* **1992**, *5*, 72.

(13) Elliott, D. C.; Phelps, M. R.; Sealock, L. J., Jr.; Baker, E. G. *Ind. Eng. Chem. Res.* **1994**, *33*, 566.

(14) Mango, F. D.; Hightower, J. W.; James, A. T. *Nature* **1994**, *368*, 536.

(15) Shock, E. L. *Nature* **1994**, *368*, 499.

(16) Seewald, J. S. *Nature* **1994**, *370*, 285.

(17) Price, L. C. *Nature* **1994**, *370*, 253.

(18) Spiess, F. N.; Macdonald, K. C.; Atwater, T.; Ballard, R.; Carranza, A.; Cordoba, D.; Cox, C.; Diaz Garcia, V. M.; Francheteau, J.; Guerrero, J.; Hawkins, J.; Haymon, R.; Hessler, R.; Juteau, T.; Kastner, M.; Larson, R.; Luyendyk, B.; Macdougall, J. D.; Miller, S.; Normark, W.; Orcutt, J.; Rangin, C. *Science* **1980**, *207*, 1421.

(19) Jones, W. J.; Leigh, J. A.; Mayer, F.; Woese, C. R.; Wolfe, R. S. *Arch. Microbiol.* **1983**, *136*, 254.

(20) Bult, C. J.; White, O.; Olsen, G. J.; Zhou, L.; Fleischmann, R. D.; Sutton, G. G.; Blake, J. A.; FitzGerald, L. M.; Clayton, R. A.; Gocayne, J. D.; Kerlavage, A. R.; Dougherty, B. A.; Tomb, J.-F.; Adams, M. D.; Reich, C. I.; Overbeek, R.; Kirkness, E. F.; Weinstock, K. G.; Merrick, J. M.; Glodek, A.; Scott, J. L.; Geoghagen, N. S. M.; Weidman, J. F.; Fuhrmann, J. L.; Nguyen, D.; Utterback, T. R.; Kelley, J. M.; Peterson, J. D.; Sadow, P. W.; Hanna, M. C.; Cotton, M. D.; Roberts, K. M.; Hurst, M. A.; Kaine, B. P.; Borodovsky, M.; Klenk, H.-P.; Fraser, C. M.; Smith, H. O.; Woese, C. R.; Venter, J. C. *Science* **1996**, *273*, 1058.

(21) Yao, J.; Evilia, R. F. *J. Am. Chem. Soc.* **1994**, *116*, 11229.

(22) Postorino, P.; Tromp, R. H.; Ricci, M. A.; Soper, A. K.; Neilson, G. W. *Nature* **1993**, *366*, 668.

(23) Tromp, R. H.; Postorino, P.; Neilson, G. W.; Ricci, M. A.; Soper, A. K. *J. Chem. Phys.* **1994**, *101*, 6210.

(24) Enderby, J. E.; Neilson, G. W. in *Water: a Comprehensive Treatise*; Franks, F., Ed.; Plenum: New York, 1979; Vol. 6, Chapter 1.

(25) Soper, A. K.; Phillips, M. G. *Chem. Phys.* **1986**, *107*, 47.

(26) Soper, A. K.; Bruni, F.; Ricci, M. A. *J. Chem. Phys.* **1997**, *106*, 247.

what constitutes a hydrogen bond.[27,28] X-ray diffraction data is also illuminating,[29-31] although X-rays do not efficiently detect the low-Z hydrogen atoms. Thus, X-ray data provide somewhat indirect evidence of H bond formation.

Another powerful technique for examining H bonds is vibrational spectroscopy, either infrared (IR) absorption[32] or Raman scattering.[33-35] Both experiments have been performed on supercritical water and reveal a red-shift upon formation of H bonds. For example, the OD vibration of HOD dilute in H_2O (to avoid resonant couplings) falls from approximately 2700 cm^{-1} in isolated molecules to nearly 2500 cm^{-1} in 25 °C water.[32,33] Vibrational spectroscopy has an additional useful feature—the spectral widths are large enough that time averaging is avoided. Thus, the observed spectrum is a superposition of the spectra of the various molecular configurations in water, as opposed to a simple Lorentzian whose center frequency reflects the time- and ensemble-average of the configurations present (e.g., as NMR does). The IR and Raman data have been analyzed to yield quantitative estimates of the extent of hydrogen bonding in supercritical water, as discussed below.[31,33] However, there is no general agreement about the analysis of the vibrational data.

Molecular dynamics simulations and Monte Carlo calculations have provided insight into hydrogen bonding.[27,28,36-38] As discussed in greater detail below, these methods generally find a reduced but non-negligible extent of H bonding in supercritical water.

In this study, we exploit the well-known, large changes in proton NMR chemical shift due to hydrogen bond formation.[1,39,40] The approximately 4.5 ppm shift[40] between water vapor and 25 °C liquid water demonstrates the large size of the effect from H bonding, when compared to the only 10 ppm range of proton shifts in all chemical compounds. The proton NMR shift has been used before to measure the changes in H bonding upon dilution[41,42] and in pure water from the super-cooled region to 120 °C.[43-45] In fact, the chemical shift variations of alcohols[46,47] and H_2O (or D_2O, used as a deuterium field frequency lock[48]) have found routine applications for thermometry in NMR experiments at modest temperatures.[49-52]

The results presented here extend this well-known technique to much higher temperatures and pressures, up to 600 °C and 400 bar (1 bar = 10^5N/m^2 = 0.987 atm), conditions well beyond the critical point. Also, the chemical shift data are analyzed to yield a quantitative measure of hydrogen bonding in the fluid. We note that the group of Nakahara[53] has made chemical shift measurements of H_2O to 375 °C. Also, Jonas and co-workers have reported the diffusion coefficient and spin—lattice relaxation of water at supercritical conditions.[54-56]

II. Experimental Section

Proton spectra of water were obtained with an NMR probe designed for this purpose. The probe is thoroughly described elsewhere;[57] in brief, the water sample is held in an alumina ceramic tube with a floating-piston device (at room temperature) to transfer the pressure from the argon gas pressurizing fluid. The hot H_2O comes into contact only with alumina ceramic, to avoid the solubility and reactivity of some other materials. The pressure vessel itself is made of titanium alloy and is internally heated. The probe is located in the room-temperature bore of a 4.4 T (186.6 MHz) superconducting magnet with adjustable room-temperature shim coils. Generally, 0.1 ppm field uniformity is attained. The NMR spectrometer is home-built. All spectra reported here are the Fourier transforms of free-induction decays following single $^\pi/_2$ pulses.

Pure water (Aldrich Chemical) was used after three freeze—pump—thaw cycles to remove dissolved gases. The water, together with a bit of solute, was then loaded into the ceramic tube/floating piston assembly. The solute was generally benzene or isopropyl alcohol, but cyclohexane and *p*-ethylphenol were occasionally used for comparisons between these reference compounds.

The solute served as an internal chemical shift reference. Thus, any changes in bulk magnetic susceptibility of the sample resulted in *equal* frequency changes of the solute and the water.[39] By measuring the frequency of the H_2O line relative to the solute resonance, only changes in *chemical shift* are measured. We note that virtually all high-resolution NMR today employs an internal lock or an internal shift standard.[48] Clearly, our internal shift standard approach is useful only if the chemical shift of the reference solute remains constant, so the observed relative frequency changes are correctly interpreted as changes in the H_2O chemical shift. This issue is addressed by experimental results (below). Here, we note that the effect upon chemical shifts of hydrogen bonding is much larger than all of the other intermolecular interaction effects (e.g., van der Waals, typically in the 0.2 ppm range).[58-60] Thus, provided the solute cannot participate in hydrogen bonding, we can safely regard the shift of the solute as a constant. The chemical shifts reported here are all determined from the frequency difference (Δf) of the water and dilute solute resonances (typically 2 mol %). The fractional shift is reported as $\Delta f/f_o$, with f_o being the frequency of either resonance. Negative shifts are for H_2O towards lower frequency (more shielded).

The temperature across the NMR active region of the sample varied by at most 2 °C. The temperatures reported here are accurate to ±3 °C, and the pressure is believed accurate to within 1%. Given the

(27) Kalinichev, A. G.; Bass, J. D. *Chem. Phys. Lett.* **1994**, *231*, 301.

(28) Chialvo, A. A.; Cummings, P. T. *J. Chem. Phys.* **1994**, *101*, 4466.

(29) Gorbaty, Yu. E.; Demianets, Yu. N. *Chem. Phys. Lett.* **1983**, *100*, 450.

(30) Yamanaka, K.; Yamaguchi, T.; Wakita, H. *J. Chem. Phys.* **1994**, *101*, 9830.

(31) Gorbaty, Yu. E.; Kalinichev, A. G. *J. Phys. Chem.* **1995**, *99*, 5336.

(32) Franck, E. U.; Roth, K. *Discuss. Faraday Soc.* **1967**, *43*, 108.

(33) Kohl, W.; Lindner, H. A.; Franck, E. U. *Ber. Bunsen-Ges. Phys. Chem.* **1991**, *95*, 1586.

(34) Ratcliffe, C. I.; Irish, D. E. *J. Phys. Chem.* **1982**, *86*, 4897.

(35) Walrafen, G. E.; Chu, Y. C.; Piermarini, G. J. *J. Phys. Chem.* **1996**, *100*, 10363.

(36) Mountain, R. D. *J. Chem. Phys.* **1989**, *90*, 1866.

(37) Fois, E. S.; Sprik, M.; Parrinello, M. *Chem. Phys. Lett.* **1994**, *223*, 411.

(38) Mizan, T. I.; Savage, P. E.; Ziff, R. M. *J. Phys. Chem.* **1996**, *100*, 403.

(39) Pople, J. A.; Schneider, W. G.; Bernstein, H. J. *High-Resolution Nuclear Magnetic Resonance*; McGraw-Hill: New York, 1959.

(40) Schneider, W. G.; Bernstein, H. J.; Pople, J. A. *J. Chem. Phys.* **1958**, *28*, 601.

(41) Cohen, A. D.; Reid, C. *J. Chem. Phys.* **1956**, *25*, 790.

(42) Harvey, J. M.; Jackson, S. E.; Symons, M. C. R. *Chem. Phys. Lett.* **1977**, *47*, 440.

(43) Hindman, J. C. *J. Chem. Phys.* **1966**, *44*, 4582.

(44) Glasel, J. A. In *Water, a Comprehensive Treatise*; Franks, F., Ed.; Plenum: New York, 1972; Vol 1, p 215.

(45) Nakahara, M. *Rev. High Pressure Sci. Tech.* **1995**, *4*, 186.

(46) Liddel, U.; Ramsey, N. F. *J. Chem. Phys.* **1951**, *19*, 1608.

(47) Arnold, J. T.; Packard, M. E. *J. Chem. Phys.* **1951**, *19*, 1608.

(48) Sanders, J. K. M.; Hunter, B. K. *Modern NMR Spectroscopy*; Oxford: New York, 1993; pp 39-41.

(49) Glew, D. N.; Mak, H. D.; McIntyre, J. S.; Rath, N. S. *Anal. Chem.* **1966**, *38*, 1964.

(50) Van Geet, A. L. *Anal. Chem.* **1970**, *42*, 679.

(51) Lutz, N. W.; Kuesel, A. C.; Hull, W. E. *Magn. Reson. Med.* **1993**, *29*, 113.

(52) Kuroda, K.; Suzuki, Y.; Ishihara, Y.; Okamoto, K.; Suzuki, Y. *Magn. Reson. Med.* **1996**, *35*, 20.

(53) Nakahara, M. Private communication.

(54) Jonas, J.; DeFries, T.; Lamb, W. J. *J. Chem. Phys.* **1978**, *68*, 2988.

(55) Lamb, W. J.; Jonas, J. *J. Chem. Phys.* **1981**, *74*, 913.

(56) Lamb, W. J.; Hoffman, G. A.; Jonas, J. *J. Chem. Phys.* **1981**, *74*, 6875.

(57) Hoffmann, M. M.; Conradi, M. S. *Rev. Sci. Instrum.* **1997**, *68*, 159.

(58) Buckingham, A. D.; Schaefer, T.; Schneider, W. G. *J. Chem. Phys.* **1960**, *32*, 1227.

(59) Howard, B. B.; Linder, B.; Emerson, M. T. *J. Chem. Phys.* **1962**, *36*, 485.

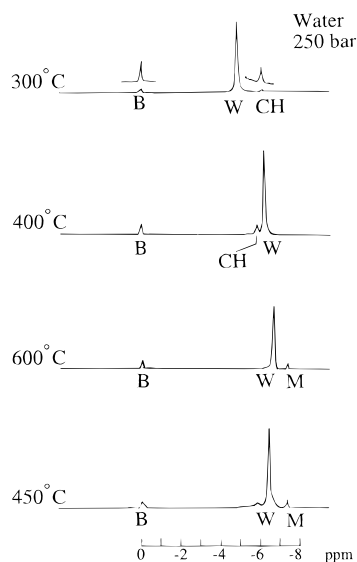(60) Bothner-By, A. A. *J. Mol. Spectrosc.* **1960**, *5*, 52.

Figure 1. Proton NMR spectra of water at 250 bar with dilute benzene and dilute cyclohexane as internal references. From top to bottom, the spectra appear in the order they were measured. The peaks are labeled W (water), B (benzene), CH (cyclohexane), and M (methane, from high-temperature decomposition). The spectra are aligned to maintain a fixed location of the benzene peak. The display gain has been increased ($\times 11$) for some of the weaker solute peaks. The down-frequency shift (to the right) of the water resonance with increasing temperature is evident.

gradual variation of chemical shift with temperature and pressure (see data below), these uncertainties are negligible.

III. Results: Chemical Shift

Typical NMR spectra of water are presented in Figure 1, where the temperature was raised to 600 °C and then decreased, all at 250 bar. Small quantities of benzene (B) and cyclohexane (CH) were present to serve as internal references of chemical shift. The concentrations of the solutes are best determined from the ratios of intensities (areas) in Figure 1, keeping in mind the numbers of hydrogens per molecule. The large temperature gradient along the ceramic sample vessel results in a nonuniform distribution of the solute throughout the vessel. The increasing solubilities of benzene and cyclohexane at elevated temperatures lead to the increasing solute concentrations apparent in Figure 1.

The down-frequency shift (to the right) of the water (W) resonance with increasing temperature is clearly evident in Figure 1. Measurement of this shift and its interpretation in terms of hydrogen bonding as a function of temperature and density constitute the subjects of this research.

The spectra in Figure 1 have been aligned (i.e., by small additive frequency shifts to correct for changes in bulk magnetic susceptibility) to keep the benzene (B) resonance at a fixed position. The cyclohexane (CH) and methane (M) lines remain at fixed positions (when visible), indicating that their shifts remain virtually constant. Further support for treating the benzene resonance as a *fixed* reference is presented below. The methane signal first becomes evident at 500 °C (not shown) and is believed to be due to chemical reaction of the cyclohexane; no methane signal was ever found with only water and benzene. When the sample was cooled from 600 °C, the methane resonance remained, as expected. At room temperature, the identity of the gas was confirmed by mass spectrometry.

Much of the data presented here used dilute benzene as an internal reference. However, at low temperatures, the low solubility of benzene in water made it advantageous to use the methyl (CH$_3$) resonance of isopropyl alcohol as a reference
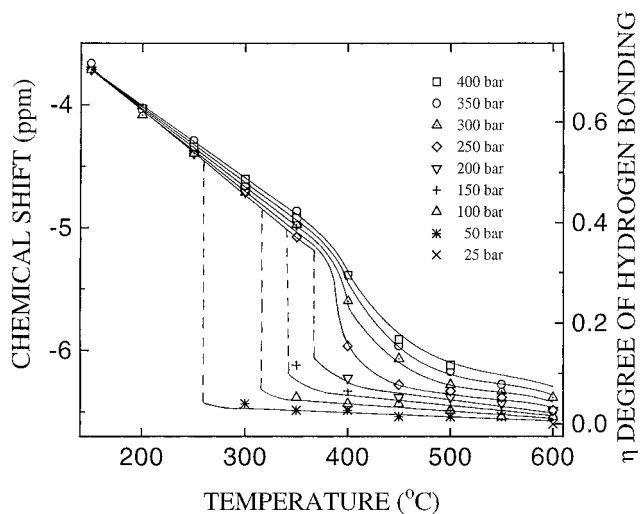

Figure 2. Chemical shift of water relative to dilute benzene as an internal reference, at several pressures. Negative shifts are to lower frequencies. The smooth curves are to guide the eyes; the dashed lines indicate the discontinuity across the liquid−vapor coexistence. The right-hand scale for η, the extent of hydrogen bonding, is linearly related to the chemical shift as explained in the text.
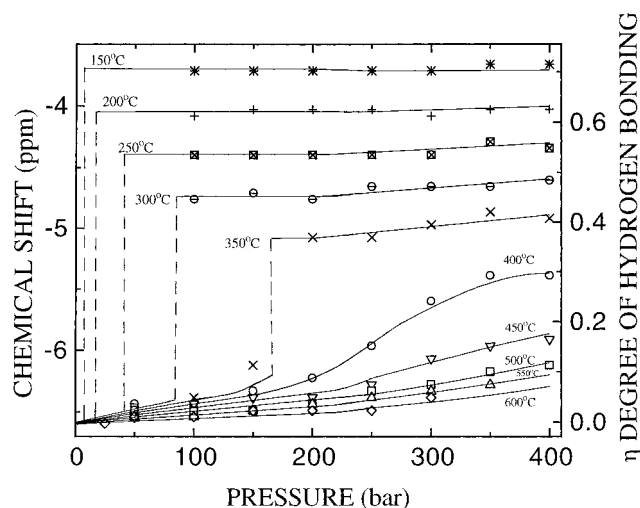

Figure 3. Pressure dependence of the chemical shift of water relative to dilute internal benzene, at several temperatures. The smooth curves are guides for the eyes; the dashed lines indicate two-phase coexistence regions. The degree of hydrogen bonding is expressed by the right-hand scale, as described in the text.

line. At high temperatures, isopropyl alcohol partially dehydrates to propene,[61] making isopropyl alcohol unsuitable as a high-temperature reference.

The chemical shift data in Figures 2−4 cover the high-temperature range and were all measured with respect to dilute internal benzene. From Figure 2, the water resonance shifts to lower frequency (i.e., more shielded) as temperature increases and the hydrogen bond network is gradually destroyed. As explicitly shown in Figure 3, the pressure dependence of the shift is quite weak over our pressure range *in the liquid range* (above the coexistence pressure, for temperature ≤350 °C). Presumably, this reflects the low compressibility of the dense liquid. Across the liquid−vapor coexistence, large changes in the chemical shift are observed (Figures 2 and 3), showing that the hydrogen bonding is substantially weaker in the less-dense vapor phase. The location of the discontinuities in shift agree with the published coexistence curve for pure water[5] to within

(61) Narayan, R.; Antal, M. J., Jr. *J. Am. Chem. Soc.* **1990**, *112*, 1927.
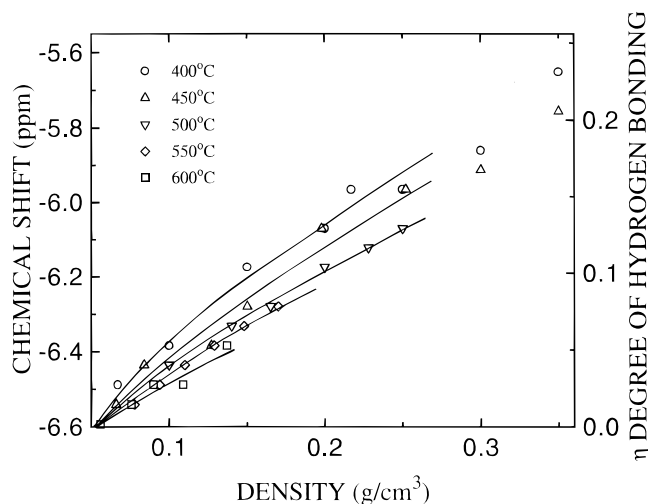
Figure 4. Density dependence of the chemical shift of water relative to internal benzene at several temperatures above the critical temperature. The five curves are eye guides for the data at low density at each temperature, in order of increasing temperature from top to bottom.

our coarse data grid, despite the presence of dilute solute. For vapor and supercritical fluid ($T > 374$ °C), the chemical shift does vary with pressure in the expected direction—increasing pressure and density result in more H bonding and an up-frequency shift (less shielded).

At high temperature and low pressure, the shift of water appears to reach a limiting value. This is made clear in Figure 4, where the shift is plotted as a function of fluid density. Within the uncertainty of the data, the shift approaches −6.6 ppm as density approaches 0. Densities were obtained from PVT data for pure water[5] and should be accurate for the present dilute solutions, except very near the critical point. As expected, the increase of the shift with density is weakest for the highest temperature, 600 °C. Because high temperature and low density both weaken the hydrogen bonding, we take −6.6 ppm shift as characteristic of H_2O monomers (i.e., unassociated) and no H bonds.

The chemical shift of liquid water for the lower temperatures (≤ 350 °C) is presented in Figure 5. There the data from three sets of research groups with various shift references are compared. First, the present results obtained with dilute internal benzene reference appear as circles. Because the data extend to 350 °C, pressure is required to retain liquid densities. We arbitrarily choose to present 250 bar data, noting the very weak pressure dependence in Figures 2 and 3 at these conditions. Because of the low solubility of benzene in cold water, these data do not extend below 150 °C. To overcome this problem, measurements were performed using the methyl resonance of dilute, internal isopropyl alcohol as the reference, both at 250 and 1 bar (squares and triangles, respectively). As expected, the data at the two pressures agree well where they overlap in Figure 5. The data referred to isopropyl alcohol were converted to the benzene reference scale using the shifts of benzene and the methyl resonance of isopropyl alcohol relative to TMS (tetramethylsilane, 7.33 and 1.20 ppm, respectively), as tabulated.[62] While the tabulated values are obtained in a solvent quite different from water, the solvent effect upon these non-hydrogen-bonding groups is expected to be small. We will return to this crucial issue below. The data with isopropyl alcohol reference, additively corrected as described above, are found in Figure 5 to be in agreement with the benzene-referenced measurements to within 0.1 ppm.
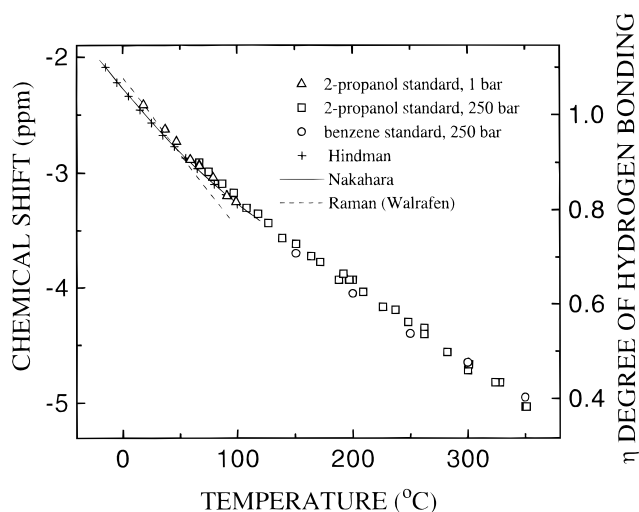
(62) Pouchert, C. J.; Behnke, J. *The Aldrich Library of ¹³C and ¹H FT NMR Spectra*, 1st ed.; Aldrich Chemical Co.: Milwaukee, WI, 1993.

Figure 5. Chemical shift of water relative to dilute internal benzene in the lower temperature (high density) region. The NMR data of Nakahara are from ref 45, and Hindman's NMR data are from ref 43. The present data obtained at 250 bar with benzene reference are shown together with 1 bar and 250 bar data taken with the methyl resonance of dilute internal isopropyl alcohol as reference. See text for conversion between the different references. The good agreement between the groups is evident. Data for η from the Raman work of ref 65 are shown.

The chemical shift of water at room pressure from Nakahara[45] appears as a solid curve in Figure 5. The curve is obtained from the empirical equation used to fit the original data. The data were referenced to TMS, so the shift of 7.33 ppm of benzene relative to TMS was used as a subtractive correction.[62] The earlier data of Hindman[43] were expressed as shift relative to water at 0 °C. The Hindman data were additively shifted by an amount selected to obtain agreement with the Nakahara data at 0 °C; this is the *only* adjustable offset in all of the data in Figure 5.

There are two major conclusions to be drawn from Figure 5. First, the data of the three NMR research groups are in remarkably good agreement. Second, as demonstrated by the agreement of shifts with different reference solutes, our procedure that assumes the chemical shifts of the solutes are constants appears to be valid.

We now turn to direct experimental tests of the validity of our use of internal reference solutes. The shift of water, measured against internal, dissolved benzene is presented in Figure 6 as a function of benzene concentration. The variations are all small, so that quite reliable "zero concentration" values may be obtained. Of course, it is possible that the water and benzene chemical shifts were affected equally by the presence of the benzene solute, but this seems unlikely, especially over the wide range of temperatures in Figure 6.

The chemical shifts of several solutes are compared in Figure 7. The shifts of methane (M) and cyclohexane (C_6H_{12}) in the figure are referenced to internal, dilute benzene, as in Figure 1. The shifts of the -CH_2- and -CH_3 groups of *p*-ethylphenol were measured relative to the ring resonances in the same compound. These values were additively corrected by the tabulated shift between the ring resonances and benzene.[62] The solute shifts are essentially independent of temperature. By comparison, the solid curve shows the large variation in the shift of the water itself. It seems extremely improbable that all of these solutes (alkyls) and benzene have nontrivial changes in chemical shift *which are all equal*. Thus, from Figures 6 and 7, we conclude that the chemical shifts of the solutes are essentially constants and that we are working in the limit of low solute concentration.
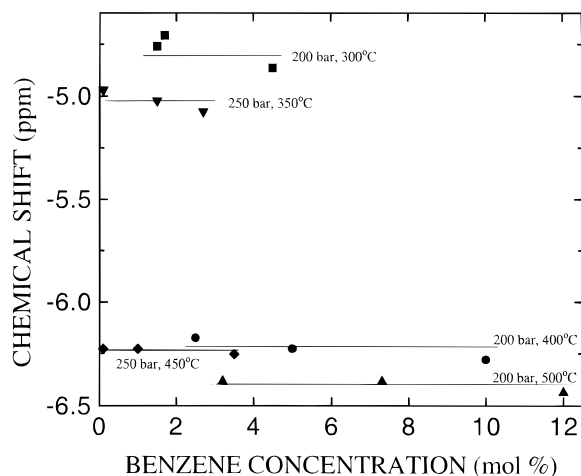
Figure 6. Dependence of the water chemical shift relative to internal benzene as a function of the concentration of the benzene. The near absence of concentration dependence allows reliable extrapolations to the infinitely dilute limit. The solid lines are eye guides.
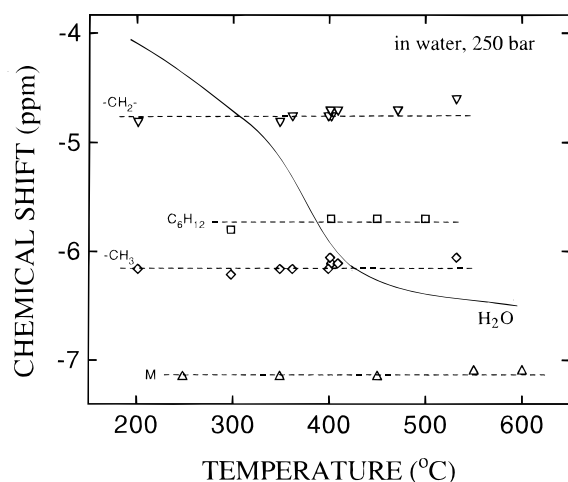

Figure 7. Chemical shifts of several dilute solutes, referred to dilute internal benzene; in all cases the medium is water at 250 bar. From bottom to top, the solute resonances are methane (M), the -CH$_3$ line of *p*-ethylphenol, cyclohexane (C$_6$H$_{12}$), and the -CH$_2$- line of *p*-ethylphenol. The constancy of the shifts of these solutes demonstrates that the solute shifts are unaffected by the changes in hydrogen bonding of the water. The straight lines are eye guides. For comparison, the curve shows the large variation of the shift of H$_2$O (data points suppressed to reduce clutter).

IV. Discussion: Hydrogen Bonding

The changes in chemical shift of the H$_2$O protons with changes in temperature and density overwhelmingly reflect the changes in hydrogen bonding.[39-41] By comparison, other influences upon the chemical shift are minor.[39,58-60] This assertion is graphically demonstrated by Figure 7, in which the non-hydrogen-bonding solute molecules show at most only small shift changes compared to the water, as the temperature of the water solvent is changed over a wide range.

The measured value of the chemical shift is a time average (or, equivalently, an ensemble average) over the multitude of configurations of the fluid. Specifically, the NMR time scale is the reciprocal of the line width and is of order 10^{-1} s, much longer than the 10^{-12} s characteristic of structural fluctuations. Thus, our NMR shift measurements extract a single number from the fluid.

We analyze the chemical shift data by a linear relation between the shift (σ) and the extent of hydrogen bonding (η).

We require that $\eta = 0$ in the limit of no H bonds, as is the case for hot, low-density vapor where σ tends to -6.6 ppm, relative to internal, dilute benzene. We set $\eta = 1$ for water at 25 °C and 1 bar, an arbitrary though convenient reference state with $\sigma = -2.5$ ppm (see Figure 5). Thus, we have

$$\eta = 0.2439\sigma + 1.610 \qquad (1)$$

The above linear relation between η and the shift σ is easily justified in a two-state model, in which hydrogen nuclei are either involved or not involved (yes/no) in a hydrogen bond. A chemical shift (σ_{yes} and σ_{no}) describes each of the two states. The measured shift σ is then the weighted average of the two limiting shifts, so that σ will be linear in the time-average number of hydrogen bonds per molecule. In more complete descriptions of H bonding than the two-state model, the linear relation between the chemical shift σ and the extent of H bonding η is not rigorous. Indeed, there is no longer an unique definition of hydrogen bonds. We will return to this point below. Nevertheless, we use the linear equation (eq 1) for our analysis because of its simplicity.

The data of Figures 2−5 are presented with chemical shift scales along the left. By means of eq 1, scales for the H-bonding extent η have been affixed along the right sides. Thus, these figures simultaneously present the principal results (chemical shift) and interpretation (in terms of H bonding) of this research.

We now compare the present results for η with previous measurements. From Figures 2 and 3, we find $\eta = 0.29$ at the supercritical conditions of 400 °C and 400 bar, a density of 0.52 g/cm^3. This is certainly a nontrivial amount of H bonding. But in their NDIS study, Postorino *et al.*[22,23] found no evidence of H bonds at 400 °C and the *higher* density of 0.66 g/cm^3. We recall from Figures 2−4 that *more* H bonding, not less, is expected at the higher density and pressure of the neutron NDIS work. We note that the NDIS results have been critiqued.[63] Also, a comparison between the data and molecular dynamics simulations finds specific disagreements.[64] The reanalysis of the NDIS data is awaited.[26] Recent low-frequency Raman measurements[35] in water at pressures of 500−2000 bar are interpreted as indicating that H bonds are largely broken down at 150−200 °C, in striking disagreement with the data of Figures 2−5.

An earlier Raman study by Walrafen and co-workers reports[65] the fraction f_B of hydrogen atoms involved in hydrogen bonds between 0 and 100 °C at 1 bar. These data have been converted to the present η scale, using $\eta = f_B/0.781$; the denominator is the value of f_B at 25 °C. These Raman-derived values appear in Figure 5 as a dotted curve. The agreement with the NMR results at 25 °C is forced, of course. The Raman data have a substantially larger temperature dependence than the NMR-derived values.

Several quantitative estimates of the extent of H bonding in supercritical water appear in the literature. These estimates, together with η values from Figures 2−4, are presented for comparison in Table 1. In each case, the reported values have been normalized to unity for 25 °C, 1 bar water.

The Raman measurements of Franck's group were reported[33] as values of K, the ratio of H-bonded to non-H-bonded hydrogen atoms. These data were obtained by a complicated fitting procedure with many parameters, such as the center frequency, width, and asymmetry of both spectral components (bonded and

(63) Löffler, G.; Schreiber, H.; Steinhauser, O. *Ber. Bunsen-Ges. Phys. Chem.* **1994**, *98*, 1575.
(64) Chialvo, A. A.; Cummmings, P. T. *J. Phys. Chem.* **1996**, *100*, 1309.
(65) Walrafen, G. E.; Fisher, M. R.; Hokmabadi, M. S.; Yang, W.-H. *J. Chem. Phys.* **1986**, *85*, 6970.

Table 1.   Degree of Hydrogen Bonding in Supercritical Water (η)

T (°C)	ρ (g/cm^3)	η	method	reference
400	0.52	0.29	NMR	this work
400	0.45	0.43	MD	Mountain, ref 36
400	0.5	0.45	theory	Johnston *et al.*, ref 66
400	0.66	negligible	NDIS	Postorino *et al.*, refs 22 and 23
400	0.66	0.5	theory	Johnston *et al.*, ref 66
400	0.75	0.66	MD	Mountain, ref 36
400	0.8	0.36	Raman	Franck *et al.*, ref 33
400	0.7−1.1	0.45	IR + X-ray	Gorbaty *et al.*, ref 31
500	0.12	0.08	NMR	this work
500	0.115	0.11	Monte Carlo	Kalinichev *et al.*, ref 27
500	0.15	0.14	MD	Mountain, ref 36
500	0.115	0.15	MD	Savage *et al.*, refs 38 and 68
500	0.115	0.16	theory	Johnston *et al.*, ref 66
500	0.20	0.13	NMR	this work
500	0.257	0.19	Monte Carlo	Kalinichev *et al.*, ref 27
500	0.25	0.23	MD	Mountain, ref 36
500	0.257	0.26	MD	Savage *et al.*, refs 38 and 68
500	0.257	0.29	theory	Johnston *et al.*, ref 66

nonbonded), separately adjustable at each temperature. The K values were converted to the number N of H bonds per H_2O molecule (on a scale where 2 is maximum) using $N = 2K/(K + 1)$. The 25 °C water had 1.73 H bonds per molecule. Finally, the data were normalized to $\eta = 1$ at 25 °C. These data are only available at high density, about 0.8 g/cm^3, and do not extend beyond 400 °C. Given the very high density, the value in Table 1 should be regarded as being in reasonable agreement with the NMR value.

Gorbaty and Kalinichev[31] have published values of the H-bonding extent (χ in their work). The values used here are from their straight line fit to both infrared data (based on the large variation in the integrated IR absorption coefficient) and to X-ray diffraction data. The data are presented only for the high densities of 0.7−1.1 g/cm^3. Simple normalization by the 25 °C value of χ yields the η values of Table 1. As expected, at the higher density of Gorbaty and Kalinichev, they find somewhat higher η values.

A lattice fluid calculation of H bonding has been published by Johnston and co-workers.[66] They report their results as "fraction of monomer", although this is not to be understood as water molecules participating in no H bonds (out of a possible four, two as donors and two as acceptors). Instead, the fraction of monomer (FM) is the fraction of non-H-bonded hydrogen atoms. Thus, these are converted to η values using $\eta = 2(1 - FM)/1.73$. Unfortunately, Johnston and co-workers do not report results at 25 °C, so the 1.73 normalization value was obtained from the work of Franck,[33] as discussed above. Similar values are deduced from the Raman value[65] of $f_B = 0.781$ (i.e., 0.781 × 2 = 1.562). These η values from Johnston run substantially above the NMR-derived values in Table 1. We note that values are presented over a wide range of temperatures and density.[66] Smits *et al.* have computed[67] the fraction of monomers in water and have compared their results to the Johnston results.

Several molecular dynamics and Monte Carlo studies have reported estimates of H bonding in supercritical water. Kalinichev and Bass[27] suggest that a combined energetic and geometric criterion (as to what *is* an H bond) yields better values of the extent of H bonding than either one alone. These workers used a TIP4P potential at 500 °C; their n_{HB} values were divided by 3.2 (the 25 °C value) for the η scale in Table 1. Mountain[36] has used a purely geometric criterion and finds n_{HB} values that

vary mostly with density and surprisingly little with temperature. The reported values of n_{HB} are divided by 1.75 (the 25 °C, $\rho = 1$ g/cm^3 value) to convert to η. In two papers, Mizan, Savage, and Ziff have reported[38,68] molecular dynamics results at 500 °C and hotter. Their values of n_{HB} are normalized by the room temperature value ($n_{HB} = 3.13$). In all cases, the molecular dynamics and Monte Carlo values exceed the present NMR values, by as much as a factor of 2 (e.g., at 500 °C).

The Monte Carlo workers have pointed out[27] that it is relatively easy to formulate a good criterion for what *is* an H bond at low temperatures. But in supercritical water, the situation appears to be better described as a broad distribution of H-bonding environments, as opposed to a bonded/non-bonded dichotomy. Thus, different criteria result in numerically different results for η from the same simulation/calculation. The question arises, then, what criterion does the NMR measurement of chemical shift employ? The chemical shift is a measure of changes in the electronic shell, driven by the proximity of H bond donors or acceptors. The chemical shift is similar to the intermolecular potential energy in this regard. Just as energetic calculations allow the energetic and geometric criteria to be compared, quantum calculations of chemical shift should reveal the chemical shift changes for specific intermolecular configurations. It is difficult to regard any one of these measures of H bonding (geometric, energetic, or chemical shift) as clearly superior to the others.[1]

We point out that the present data can be used for comparison to predictions of the chemical shift from Monte Carlo or molecular dynamics (MD) calculations. In fact, Svishchev and Kusalik[69] have done such a comparison from their MD simulations, but limited to temperatures ≤100 °C. In general, Monte Carlo or MD can generate a large set of molecular configurations of the fluid. Because one desires only a "Boltzmann-weighted market-basket of configurations," Monte Carlo may prove to be more efficient (i.e., time evolution of the configurations is not important). The chemical shift of each hydrogen nucleus would be calculated for each configuration using a quantum chemistry computer code, for example, or the simpler technique of Svishchev and Kusalik[69] using the effect of electric fields upon the chemical shift.[70] The final step would be to average the shifts over time and over the many molecules in the simulation. Comparison of such predicted chemical shifts with the present experimental results could validate the intermolecular potential employed in the simulation. Most importantly, such a scheme could be used to tie together such disparate measures of H bonding as radial distribution functions and chemical shift.

V. Conclusions

The chemical shift of water is reported from 25 to 600 °C and from 1 to 400 bar, a range extending well beyond the critical point. The technique of an internal chemical shift standard was employed to eliminate the influence of the bulk magnetic susceptibility. Data are presented to demonstrate that the reference solutes employed here were in the infinitely dilute limit. Further, the excellent agreement between different solute resonances shows that the solute chemical shifts were essentially constant, with only the H_2O shift varying with changes in temperature and pressure.

(66) Gupta, R. B.; Panayiotou, C. G.; Sanchez, I. C.; Johnston, K. P. *AIChE J.* **1992**, *38*, 1243.

(67) Smits, P. J.; Economou, I. G.; Peters, C. J.; Arons, J. d. S. *J. Phys. Chem.* **1994**, *98*, 12080.

(68) Mizan, T. I.; Savage, P. E.; Ziff, R. M. in *Innovations In Supercritical Fluids: Science and Technology*; Hutchenson, K. W., Foster, N. R., Eds.; ACS Symposium Series 608; American Chemical Society: Washington, DC, 1995; pp 47−64.

(69) Svishchev, I. M.; Kusalik, P. G. *J. Am. Chem. Soc.* **1993**, *115*, 8270.

(70) Buckingham, A. D. *Can. J. Chem.* **1960**, *38*, 300.

The changes in H_2O chemical shift are interpreted using a linear relation between shift and the extent of H bonding. Such a linear relation is predicted in a two-state (bonded/non-bonded) model of hydrogen bonding. For the more complex situation in real water, the linear relation cannot be justified rigorously but is certainly the simplest approach. Using the linear scale, all of the measurements here yield values of the extent of hydrogen bonding (η). In particular, the H bonding in supercritical water at 400 °C and 400 bar ($\rho = 0.52$ g/cm^3) is 29% of that in ordinary water (25 °C, 1 bar). This is in sharp contrast to a recent neutron diffraction/isotopic substitution study which found no remaining hydrogen bonds, even at somewhat higher density ($\rho = 0.66$ g/cm^3, $T = 400$ °C). The NMR results are in fair agreement with molecular dynamics calculations and with combined diffraction and vibrational spectroscopic data.